Dalton Transactions

PAPER

View Article Online
View Journal | View Issue

Cite this: *Dalton Trans.*, 2018, **47**, 16627

Synthesis of tetraarylborates *via* tetralithio intermediates and the effect of polar functional groups and cations on their crystal structures†

Patryk Tomaszewski,[a] Marcin Wiszniewski,[a] Janusz Serwatowski,[a] Krzysztof Woźniak,[b] Krzysztof Durka[a] and Sergiusz Luliński*[a]

Received 10th October 2018,
Accepted 30th October 2018

DOI: 10.1039/c8dt04068k

rsc.li/dalton

A novel general protocol for the preparation of functionalized (COOH, CHO, C(O)NH*t*Bu, $B(OH)_2$) tetraphenyl- and tetrakis(4′-biphenylyl)borates is reported. It involves four-fold halogen–lithium exchange in potassium tetrakis(iodophenyl)borates and tetrakis(4′-bromobiphenylyl)borate) using *t*-BuLi in THF at −78 °C followed by treatment of the resulting tetralithio intermediates with electrophiles (CO_2, DMF, *t*-BuNCO, $B(OMe)_3$). X-ray crystal structures of ammonium tetrakis[4-(dihydroxyboryl)phenyl]borate, lithium tetrakis(3-carboxyphenyl)borate, and lithium tetrakis[4-(*tert*-butylcarbamoyl)phenyl]borate were determined showing a strong effect of the cation and polar functional group on supramolecular architecture.

Introduction

Tetraarylborates constitute an important class of compounds due to their widespread use in various fields including analytical chemistry (as components of ion-selective electrodes),[1–3] organic synthesis (as donors of the nucleophilic aryl group)[4–7] and homogeneous catalysis (as weakly coordinating anions for stabilization of active cationic metal centres).[8–10] Due to their high tetrahedral symmetry and strong tendency to form diamondoid-type structures, they have also found applications in crystal engineering,[11–13] supramolecular chemistry[14,15] and materials science. For instance, interesting polymer networks based on tetraarylborates were developed recently as single-ion conducting solid electrolytes.[16] Hence, the development of new simple general synthetic routes to functionalized tetraarylborates is an important task. Classical synthetic routes to tetraarylborates involve transmetalation of aryllithium or arylmagnesium compounds with boron compounds (such as boron halides, trialkylborates or $NaBF_4$).[17–20] However, this approach significantly limits access to derivatives bearing many popular functional groups attached to the aryl ring. Alternative strategies relying on post-synthetic modifications of tetraarylborate cores are scarce. A palladium-catalyzed cyanation[21] and Sonogashira coupling[16] of tetra(4-iodophenyl)borate (**3**) should be noted as examples of this approach. In this contribution, we present a method based on the conversion of halogenated tetraarylborates into respective lithiated intermediates using halogen–lithium exchange. The synthesis and reactivity of related lithiated arylboronates as convenient intermediates for the preparation of functionalized arylboronic acids and boron heterocycles were already reported.[22–24] This methodology was extended by our group in order to obtain selected heteroleptic diarylborinic 8-oxyquinolinates.[25] Now we demonstrate that tetralithiated tetraarylborates can be easily generated in good yields and subsequently converted into respective derivatives bearing pendant carboxyl, formyl, amido, and boronic groups. It should be noted that these compounds can be regarded as anionic analogues of tetraphenylmethane and tetraphenylsilane derivatives which were already explored as important starting materials for various applications with a special emphasis on crystal engineering[26] and for the preparation of three-dimensional covalent organic frameworks (COFs).[27,28] Thus, we discuss herein the crystal structures of the three obtained compounds with a special emphasis on the effect of cation-framework interactions on the supramolecular assembly.

[a]*Warsaw University of Technology, Faculty of Chemistry, Noakowskiego 3, 00-664 Warsaw, Poland. E-mail: serek@ch.pw.edu.pl*
[b]*University of Warsaw, Biological and Chemical Research Centre, Żwirki i Wigury 101, 02-089 Warsaw, Poland*

†Electronic supplementary information (ESI) available. CCDC 1840090, 1868753 and 1868754. For ESI and crystallographic data in CIF or other electronic format see DOI: 10.1039/c8dt04068k

Results and discussion

The synthesis of halogenated potassium tetraarylborates **1–4** was initially performed according to reported procedures.[7] Thus, respective halogenated phenyllithiums were treated with

$BF_3{\cdot}Et_2O$ in Et_2O at −78 °C in a ratio of *ca.* 5 : 1 followed by slow warming of the solution to room temperature and subsequent workup. This approach failed in the case of **5** as the reaction of 3-bromo-5-fluorophenyllithium with $BF_3{\cdot}Et_2O$ proceeds in two steps. At lower temperatures (up to *ca.* 0 °C), an initially formed aryltrifluoroborate anion is relatively inert. Thus, nucleophilic substitution of fluorine ligands occurs sluggishly so that formation of the desired product is preceded by extensive degradation of the aryllithium species upon warming the reaction mixture. Compound **5** was successfully prepared using BCl_3 as the boron source.[29] According to our observation, the reaction occurs in two steps, too. The first one involves the rapid formation of lithium (3-bromo-5-fluorophenyl)trichloroborate upon addition of a solution of BCl_3 in hexane to the solution of aryllithium at −78 °C. The substitution of chlorine atoms starts at *ca.* −30 °C as indicated by a strong exothermic effect. When a suspension of the latter lithium salt (obtained from the reaction of aryllithium with BCl_3 in the molar ratio 1 : 1) was allowed to warm above −30 °C, a similar exothermic process was observed. ^1H and ^{11}B NMR analyses of the isolated solid revealed the formation of **5**. This indicates that the intermediate aryltrichloroborate anion undergoes ligand redistribution processes under mild conditions which kinetically favours the formation of **5**. The use of BCl_3 instead of $BF_3{\cdot}Et_2O$ has also an additional advantage as the byproduct LiCl is easily removed during aqueous workup, whereas LiF forms a gelatinous phase which poses significant problems during filtration. Thus, the syntheses of **1–4** were repeated using BCl_3 resulting in improved yields in comparison with protocols based on $BF_3{\cdot}Et_2O$. In addition, a new compound **6** bearing longer 4-biphenylyl arms was successfully prepared (Scheme 1).

In the next step, halogenated potassium tetraarylborates were subjected to halogen–lithium exchange reactions leading to respective lithiated intermediates. It is critical to use rigorously dried salts to avoid undesired *in situ* protonation of Ar–Li bonds. Thus, prior this step the compounds **1–6** were heated at 150 °C under high vacuum (10^{-4} Torr) for 1 hour and then dissolved in dry THF. A solution of a halogenated tetraarylborate was then added to a solution of *t*BuLi/THF (10 equiv.) at −78 °C. In general, an immediate reaction was observed as indicated by the formation of a coloured slurry (yellow, green or grey-violet, depending on the starting material). A mixture containing the lithiated intermediate **1-Li–6-Li** was stirred for 2 h at −78 °C to complete the reaction. Then, addition of the electrophile (CO_2, DMF, *t*BuNCO or $B(OMe)_3$) followed by hydrolysis gave rise to a respective tetraarylborate bearing the carboxyl, formyl, amido or boronic functional group. In some cases, the exchange of the cation was performed in order to facilitate product isolation. It should be noted that the synthesis of **3b** from the reaction of 1-bromo-4-(dimethoxymethyl) benzene with *n*BuLi in THF/Et_2O followed by addition of BCl_3 (0.2 equiv.) was attempted. However, acid hydrolysis and workup resulted in 4-formylphenylboronic acid as a sole isolable product. The substituted tetraarylborates were isolated in the form of lithium, potassium or ammonium salts as white solids. Unfortunately, the analysis of products obtained from halogenated tetraarylborates **1**, **2** and **5** showed that they are not sufficiently pure, presumably due to an incomplete exchange of bromine atoms. Thus, one can recommend the

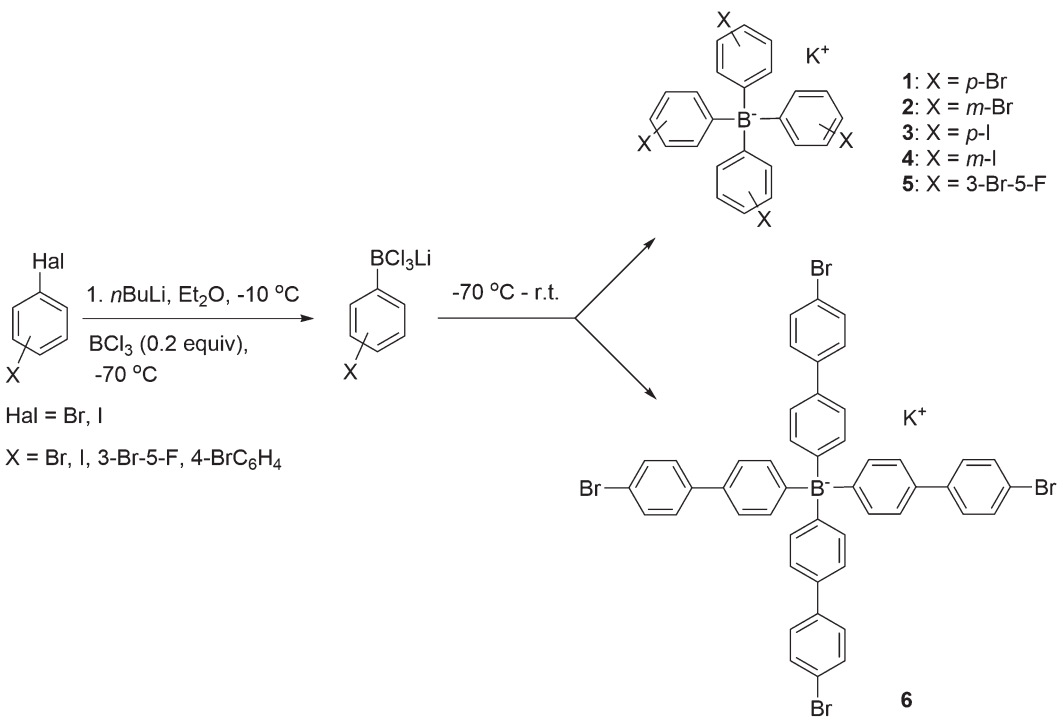

Scheme 1 Synthesis of halogenated tetrarylborates **1–6**.

use of more reactive tetra(iodophenyl)borates **3** and **4** for successful preparation of respective functionalized derivatives. On the other hand, bromine–lithium exchange occurred effectively in the case of tetrakis(4′-bromobiphenylyl)borate **6** as evidenced by high yield formation of compounds **6a–f**. The higher reactivity of **6** when compared to **1–2** can be explained in terms of a more effective separation of the negative charge in **6-Li** gradually increasing within the entire tetraarylborate scaffold upon consecutive formation of carbanionic centres.

All the obtained compounds were fully characterized by multinuclear NMR spectroscopy. ^{1}H and ^{13}C NMR spectra confirmed their structural formulation. ^{11}B NMR spectra showed a signal of the tetra-coordinate boron atom in the range of −6 to −7 ppm. In addition, we would like to raise the stability issue of the majority of obtained products under relatively strong acidic conditions. For example, derivatives bearing carboxyl groups survive at a pH of *ca.* 1 (simply estimated by the litmus paper test) for at least several hours at room temperature without any significant degradation. This allows for a convenient isolation of fully protonated forms of **3a**, **4a** and **6a** in good yields. It is well known that many tetraarylborates undergo degradation at pH < 2–3 due to the protonolysis of a B–C bond.[30] The increased protonolytic stability of the obtained compounds is beneficial from the point of view of applications which would involve the use of acidic reagents or catalysts (Schemes 2 and 3).

Structural analysis

Single crystals of **3c**, **3d** and **4a** were grown by slow evaporation of their wet acetone solutions. The ammonium salt **3d** crystallizes as a tetrahydrate in the non-centrosymmetric *Pnn*2 space group. In turn, compounds **3c** and **4a** adopt the centrosymmetric $P2_1/c$ space group (**4a** described in the $P2_1/n$ setting) and incorporate lithium counterions into their structures. Thus, it is expected that structures of lithium and ammonium salts would vary significantly due to different coordination modes of respective cations. Since the binding in lithium coordination compounds is predominately electrostatic in nature and the Li^+ radius is of only 0.6 Å, its tetrahedral complexation with hard bases is strongly preferred.[31] In the case of ammonium salts, the charge-supported hydrogen bonds with boronic groups could be expected but structural analysis of **3d** revealed preference for interaction of the NH_4^+ cation with the aromatic π-cloud.[32,33] Consequently, such interactions symmetrically connect four aromatic rings from two neighbouring anions of **3d** (Fig. 1a). Due to these interactions, the anion is significantly distorted from the general T_d symmetry with the rather small (102.6(8)°) C–B–C angle between the aromatic rings sharing the same cation. The propagation of this motif along the [010] direction results in the formation of a one-dimensional cation–anion string, which resembles the structural motif found in unsubstituted ammonium and alkaline metal tetraphenylborates.[13] The distance of the nitrogen atom to the aromatic ring centroid equals to 3.12(2) Å and is slightly longer than that in NH_4BPh_4 (3.048 Å).[32] Boronic groups are linked *via* pairs of O–H···O hydrogen-bond interactions forming centrosymmetric dimers commonly encountered in crystal structures of boronic acids.[34,35] However, in **3d** the *p*-$(HO)_2BC_6H_4$ groups from adjacent anions are not aligned in the same plane (the average distance between mean planes of corresponding aromatic rings is 2.05(2) Å) (Fig. 1b). It is also noticeable that the entire group is significantly bent out of its mean plane which is the result of NH_4^+···C(π) and boronic group hydrogen-bond interactions. Since each anion forms four hydrogen-bond connections to the neighbours, the structure extends to the three-dimensional diamondoid-type network. It is significantly elongated in the [010] direction reflecting the distortion of molecular geometry (Fig. 2a and b). Furthermore, the structure shows a six-fold interpenetration level (Fig. 2c). Compared to related structures of neutral tetraboronic acids based on tetraphenylmethane and tetraphenylsilane backbones,[26] where five-fold interpene-

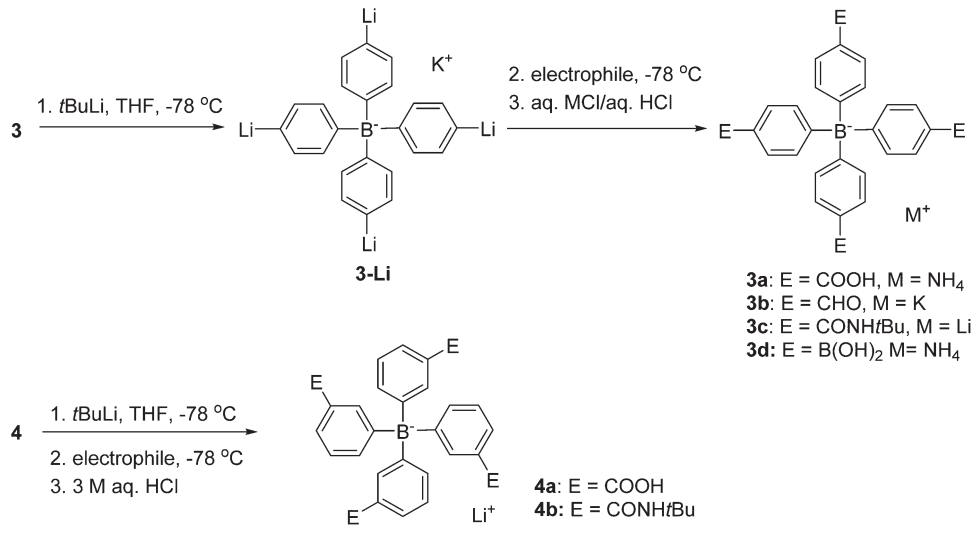

Scheme 2 Synthesis of functionalized tetraphenylborates.

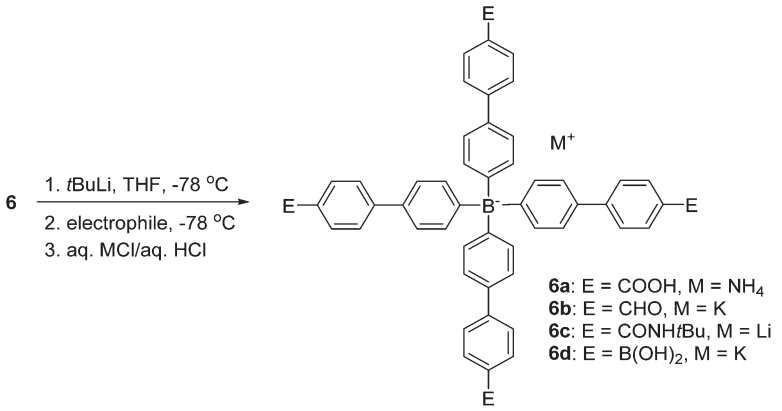

Scheme 3 Synthesis of functionalized tetrakis(4′-biphenylyl)borates.

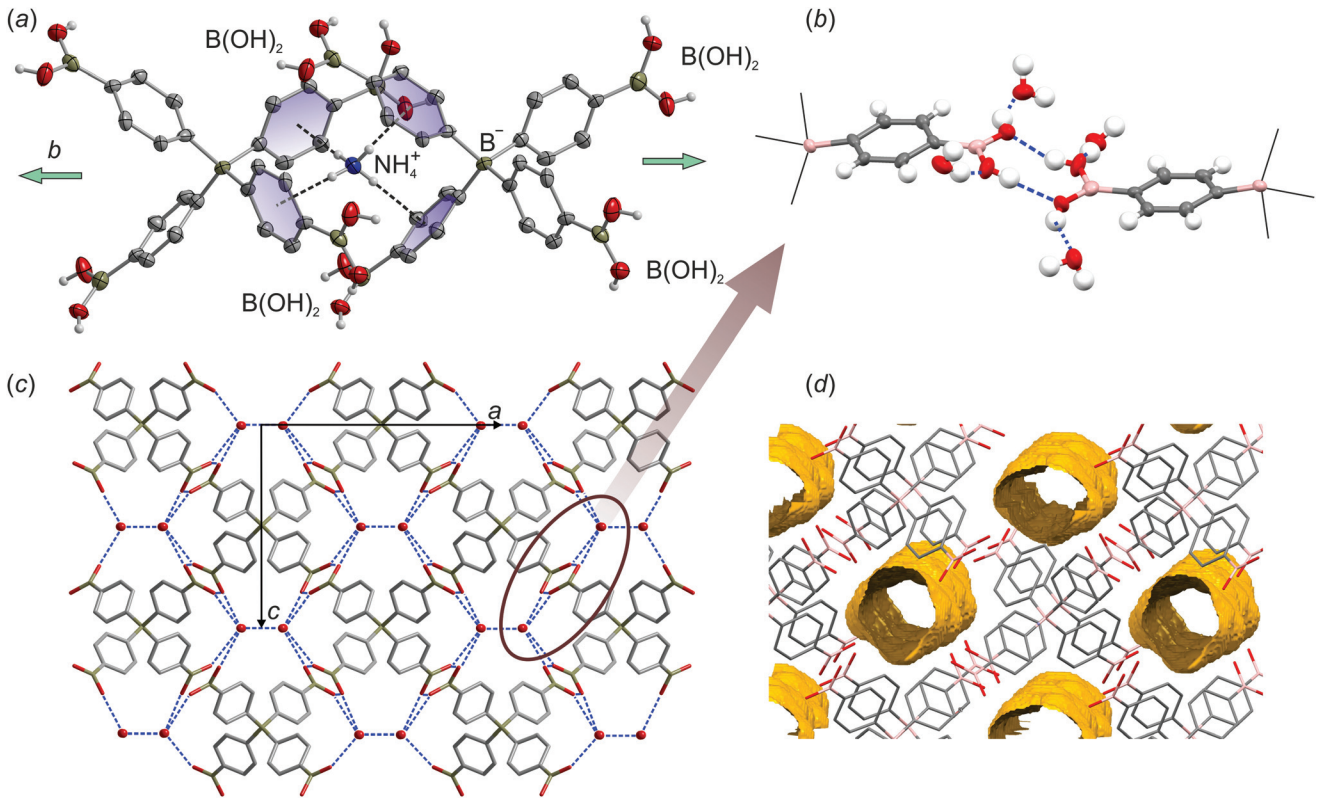

Fig. 1 Two main structural motifs governing the molecular organization in **3d**: (a) $NH_4^+\cdots C(\pi)$ cation–anion chains, (b) hydrogen bonds formed between boronic groups and water molecules, (c) hydrogen bond network formed with boronic groups and water molecules. Thermal motions are shown as atomic displacement parameters (ADPs) at the 50% probability level. (d) The visualization of crystal voids (water molecules were excluded from the structure).

tration was observed, the packing of **3d** has a higher interpenetration level due to significant structure elongation which allows for the insertion of one additional network. The interpenetrating networks are not independent of each other as they are held by the $NH_4^+\cdots C(\pi)$ interactions. Another important difference is the increased compacity of the ionic tetraboronic structure. Both types of structures possess the volume available for inclusion of guest molecules. However, in **3d** it comprises only 14% of the total unit cell volume, whereas in neutral tetraboronic acids nearly 60% of the total crystal volume are available for guest molecules. Furthermore, the channels in **3d** are aligned in the [010] direction and are not connected one with another (Fig. 1d). Since the structure was obtained by crystallization from wet acetone solution, the channels are filled with water molecules which form well-defined O–H···O interactions with boronic groups (Fig. 1c). In

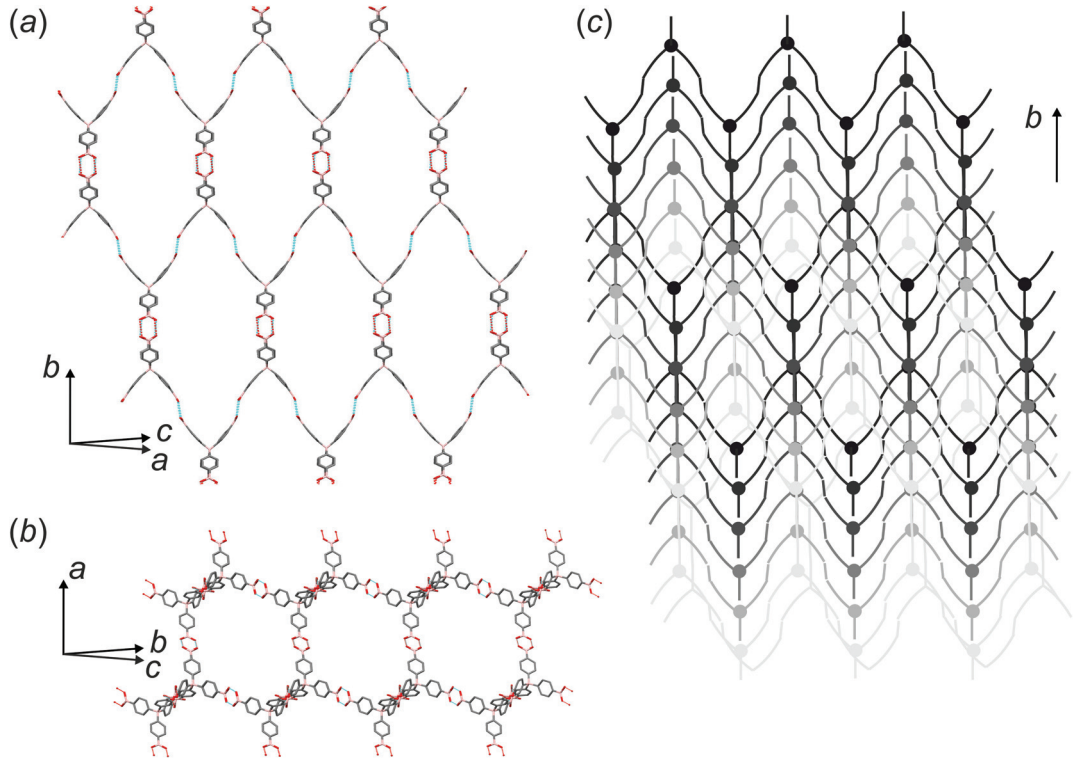

Fig. 2 Distorted diamondoid-type hydrogen-bonded network viewed parallel to (a) [010] and (b) [100] directions. (c) Graphical representation of the six-fold network interpenetration in **3d**.

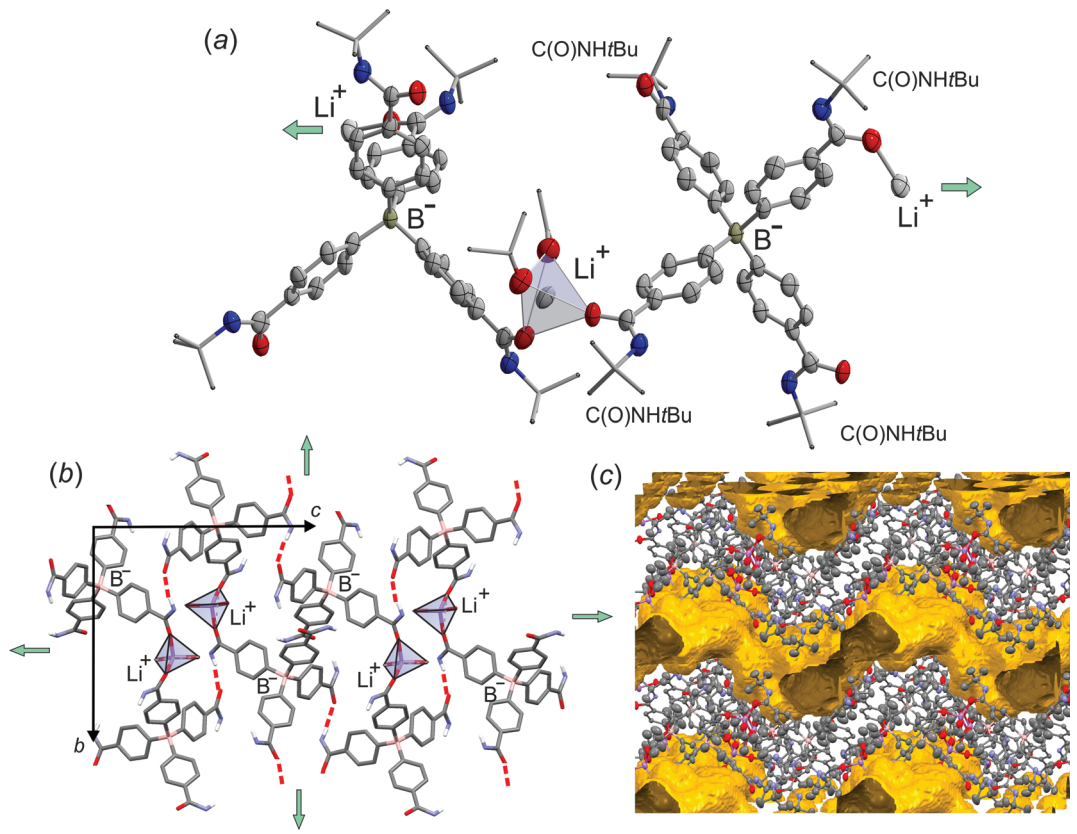

Fig. 3 (a) Molecular structure of **3c**. Thermal motions given as ADPs at the 50% probability level. (b) Fragment of the crystal structure of **3c** showing the formation of the (100) molecular layer. (c) The visualization of crystal voids (solvent molecules were excluded from the structure).

summary, the supramolecular structure of **3d** can be described as the 6-fold interpenetrated distorted diamondoid-type network formed by two different structural motifs originating from hydrogen-bonds between boronic groups as well as $NH_4^+\cdots C(\pi)$ interactions.

In contrast to **3d**, the crystal structure analysis of **3c** and **4a** shows that coordination of lithium cations by oxygen atoms (either from the acetone or amide group) is preferred for $Li^+\cdots C(\pi)$ interactions. Thus, the molecular geometries are not strongly affected by intermolecular interactions and adopt well-defined tetrahedral symmetry. In the case of **3c**, the Li^+ cation is coordinated by oxygen atoms from two amide groups and two acetone molecules (Fig. 3a). The oxygen atoms from two remaining amide groups play a role of acceptors in N–H···O hydrogen bond interactions. It means that there are an insufficient number of hydrogen-bond acceptors and thus two N–H groups remain free. Despite the tetrahedral symmetry of the anion, structural propagation through N–H···O hydrogen bonds and Li^+-centred tetrahedra is restricted to (100) planes (Fig. 3b), whereas interactions between such layers are mainly of the van der Waals nature. The structure possesses nearly 17% of crystal voids (Fig. 3c). They are enclosed in the form of bubbles connected in a waved surface parallel to the (100) plane, thus partially separating the molecular planes and weakening their mutual interactions. The cavities are filled with disordered acetone molecules. Despite the presence of free N–H hydrogen bond donors, the solvent molecules are not involved in any interactions with these groups.

Unfortunately, we did not manage to obtain a single crystal of the *para*-substituted tetracarboxylic derivative **3a**; however, its *meta* analogue **4a** was successfully characterized (Fig. 4a). This is somewhat in contrast to our expectations, as crystal structures of related neutral compounds tetrakis(4-carboxyphenyl)methane and tetrakis(4-carboxyphenyl)silane were reported and widely discussed,[36–38] while their *meta* isomers have not been published, so far. The crystal structure of **4a** seems not to be affected by ionic nature of this compound, as (1) the lithium cation was found to be disordered over four positions residing in the crystal cavity, (2) it is weakly solvated by the inserted solvent molecules, (3) it is not involved in any

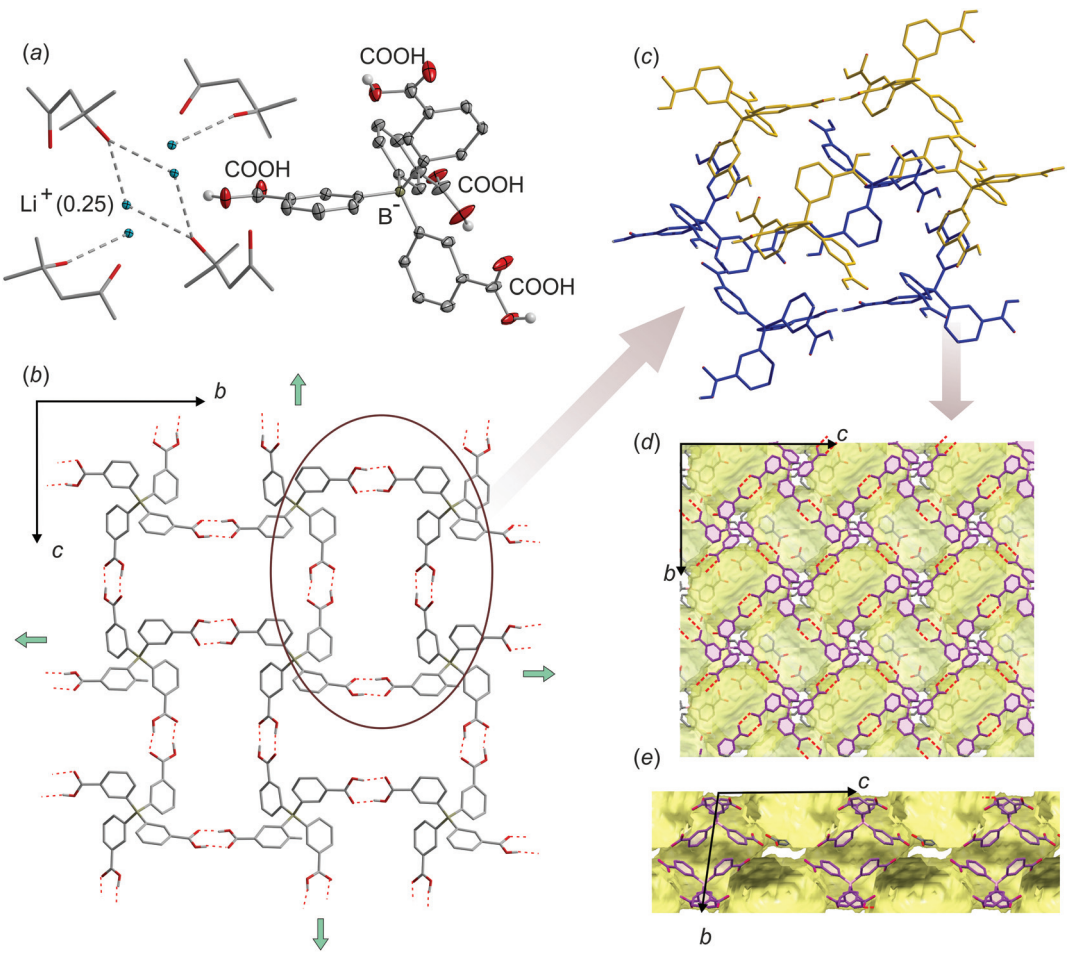

Fig. 4 (a) Molecular structure of **4a** with ADPs defined at 30% probability level. Solvent molecules are presented in capped stick style for clarity. (b) Hydrogen-bonded (100) layer resulted from mutual COOH···HOOC interactions. (c) Disposition of two hydrogen-bonded tetrameric motifs from neighbored layers (drawn in yellow and blue colors, respectively) defining the crystal cavity. (d, e) Void surface generated for hydrogen-bonded anionic framework (solvent molecules and Li^+ cations were extruded from the structure).

interaction with the hydrogen-bonded framework, and (4) molecular aggregation mostly results from the H-bonding interactions of carboxylic groups. The mutual COOH···HOOC hydrogen-bonds lead to the formation of a cyclic tetrameric motif. It adopts a rectangular shape and boat conformation (Fig. 4b and c). Each anion shares four such structural motifs; however, their propagation is restricted to *b* and *c* directions. Consequently, herring-bone arrangement in the (100) layer is observed. The layers are mostly held by π-stacking and the C–H···π(C═O) interactions operating along the [100] direction. In contrast to **3d**, the structure **4a** is not affected by the interpenetration. Two hydrogen-bonded tetramers from neighboured layers enclose the spherical cavity (Fig. 4c). They are interconnected through the narrow necks of approximately 5 Å diameter and comprise 51% of the unit cell volume (Fig. 4d and e). They are filled with Li^+ cations coordinated with oxygen atoms of 4-hydroxy-4-methylpentan-2-one, and presumably 4-methylpent-3-en-2-one along with acetone (the exact composition is not clear as solvent molecules are disordered and can share the same position). The appearance of higher molecular weight compounds apparently results from the aldol-type self-condensation reaction of acetone.

Conclusions

In conclusion, optimization of the synthesis of halogenated tetraarylborates **1–6** revealed that using BCl_3 is more advantageous than using $BF_3{\cdot}Et_2O$ as the substitution of chlorine atoms occurs quantitatively under milder conditions compared to the substitution of fluorines. Regarding subsequent halogen–lithium exchange, the use of more reactive iodinated tetraphenylborates proved to give optimal results. The generated tetralithiated tetraarylborates were successfully treated with electrophiles such as CO_2, DMF, *t*BuNCO, and $B(OMe)_3$ to furnish a series of novel tetraarylborates. We expect that derivatization of the described tetrakis(lithioaryl)borate reagents with other electrophiles may provide a wide and convenient access to various functionalized tetraarylborates, otherwise not easily accessible.

The structural analyses show the ambivalent influence of cations on the topology of the obtained hydrogen-bonded anionic frameworks. This is represented by the three studied examples where such an effect is revealed at three different levels of supramolecular organization. In the case of **3c**, the lithium cations are coordinated by amido groups and thus directly participate in the formation of molecular layers. The network of ammonium salt **3d** is based on the hydrogen-bond interactions between the boronic groups resulting in diamondoid topology. However, due to $NH_4{\cdots}C(\pi)$ interactions the anions of **3d** deviate from the tetrahedral geometry, which, in turn, leads to a significant elongation of the network. This results in a higher level of network interpenetration and more compact character of the structure in comparison with neutral tetraboronic analogs. In the extreme example of **4a**, the structure is dominated by the hydrogen-bond interactions formed between the carboxylic groups, while lithium cations reside in the structural cavities solvated by the included guest molecules and do not participate in supramolecular assembly of the anionic framework.

Finally, we would like to stress that the obtained compounds are potentially interesting for a variety of applications. The work on the preparation of ionic covalent organic frameworks, coordination polymers and other microporous materials using the obtained compounds as key substrates is currently in progress by our group. In addition, the use of selected functionalized tetraarylborates in the construction of electrochemical sensors can also be envisioned.

Experimental section

General comments

All reactions involving air and moisture sensitive reagents were carried out under an argon atmosphere. Et_2O and THF were purified by refluxing with benzophenone ketyl and freshly distilled prior to use. Starting materials: dihalobenzenes, 4,4′-dibromobiphenyl, *n*BuLi (2 M solution in hexanes), *t*BuLi (1.7 M in pentane), $BF_3{\cdot}Et_2O$, and BCl_3 (1 M solution in hexane) and other important reagents including *N*,*N*-dimethylformamide, *tert*-butyl isocyanate, and trimethoxyborane were received from Aldrich. The NMR chemical shifts are given relative to TMS using known chemical shifts of residual proton (^1H) or carbon (^{13}C) solvent resonances. ^{11}B chemical shifts were given relative to $BF_3{\cdot}Et_2O$. The synthesis of lithium salts with tetrakis(halophenyl)borate anions of **1–4** was reported previously.[20,21]

Synthesis

Potassium tetrakis(4-bromophenyl)borate (1). 1,4-Dibromobenzene (23.6 g 100 mmol) was dissolved in Et_2O (150 mL). The solution was cooled to −40 °C and 2 M *n*-BuLi (50 mL, 100 mmol) was added dropwise while maintaining the temperature below −30 °C. The resulting slurry was stirred for 1 h at −40 °C and then cooled to −78 °C. Then a 1 M solution of BCl_3 in hexane (20 mL, 20 mmol) was added dropwise. A cooling bath was removed and the mixture was allowed to warm to room temperature and left overnight. Solvents were evaporated under reduced pressure and the solid residue was treated with a solution of aqueous KCl (5 g in 50 mL of water). The crude product was filtered, washed with water (3 × 50 mL) and DCM (2 × 25 mL) and dried under reduced pressure. The dried product was dissolved in THF (100 mL). The resulting solution was filtered and evaporated. The pure anhydrous product was obtained by heating for 2 h at 150 °C under high vacuum (10^{-4} Torr). White powder, dec. >356 °C, yield: 14.0 g (84%). ^1H NMR (400 MHz, acetone-d_6) δ 7.14–7.12 (m, 16H) ppm; ^{13}C NMR (101 MHz, acetone-d_6) δ 161.2 (q, J_{BC} = 49.6 Hz), 137.7 (q, J_{BC} = 1.6 Hz), 128.4 (q, J_{BC} = 3.0 Hz), 116.2 ppm. ^{11}B NMR (96 MHz, acetone-d_6) δ −7.5 ppm.

Potassium tetrakis(3-bromophenyl)borate (2). This compound was obtained as described for **1** starting with 1,3-dibro-

mobenzene (13.3 g, 56.3 mmol). White powder, dec. >332 °C, yield: 7.4 g (92%). ^{1}H NMR (400 MHz, acetone-d_6) δ 7.42–7.38 (m, 4H), 7.23–7.18 (m, 4H), 7.09–7.05 (m, 4H), 7.01–6.98 (m, 4H) ppm; ^{11}B NMR (96 MHz, acetone-d_6) δ −6.97 ppm; ^{13}C NMR (100 MHz, acetone-d_6), δ 165.5 (q, J_{BC} = 49 Hz), 137.7 (q, J_{BC} = 1.7 Hz), 134.3 (q, J_{BC} = 1.2 Hz), 127.9 (q, J_{BC} = 3.0 Hz), 125.5, 121.4 (q, J_{BC} = 3.7 Hz) ppm.

Potassium tetrakis(4-iodophenyl)borate (3). This compound was obtained as described for **1** starting with 1,4-diiodobenzene (33.0 g, 100 mmol). White powder, dec. >355 °C, yield: 20.5 g (90%). ^{1}H NMR (400 MHz, acetone-d_6) δ 7.31 (dd, J = 8 Hz, 8H), 6.93–6.88 (m, 8H) ppm; ^{13}C NMR (101 MHz, acetone-d_6) δ 161.7 (q, J_{BC} = 49.5 Hz), 138.3 (q, J_{BC} = 1.5 Hz), 134.5 (q, J_{BC} = 2.9 Hz), 87.6 ppm. ^{11}B NMR (96 MHz, acetone-d_6) δ −7.5 ppm.

Potassium tetrakis(3-iodophenyl)borate (4). This compound was obtained as described for **1** starting with 1,3-diiodobenzene (16.5 g, 50 mmol). White powder, dec. >350 °C, yield: 9.5 g (88%). ^{1}H NMR (300 MHz, acetone-d_6) δ 7.67–7.61 (m, 4H), 7.28 (ddd, J = 5.4, 2.7, 1.2 Hz, 4H), 7.23 (dddd, J = 8.7, 3.8, 2.5, 1.2 Hz, 4H), 6.90–6.82 (m, 4H) ppm; ^{13}C NMR (101 MHz, acetone-d_6) δ 165.9 (q, J_{BC} = 49.2 Hz), 144.0 (q, J_{BC} = 1.6 Hz), 134.8 (q, J_{BC} = 1.3 Hz), 131.3, 128.3 (q, J_{BC} = 2.9 Hz), 94.8 (q, J_{BC} = 3.8 Hz) ppm. ^{11}B NMR (96 MHz, acetone-d_6) δ −7.27 – −7.33 (m) ppm.

Potassium tetrakis(3-bromo-5-fluorophenyl)borate (5). This compound was obtained as described for **1** starting with 1,3-dibromo-5-fluorobenzene (25.5 g, 100 mmol). During the addition of BCl_3 (1 M solution in hexane, 25 mL, 25 mmol) the temperature was kept below −70 °C. Then, the cooling bath was removed and the mixture was allowed to warm slowly. When the temperature increased to *ca.* −30 °C, the exothermic process started and the flask was placed again in the cooling bath. The temperature was kept below −20 °C for 30 min. Then the temperature was kept below −10 °C for 40 min. Further workup was carried out as described for **1**. White powder, dec. >360 °C, yield: 14.5 g (78%). ^{1}H NMR (400 MHz, acetone-d_6) δ 7.18–7.14 (m, 4H), 6.98–6.93 (m, 4H), 6.90–6.84 (m, 4H) ppm; ^{11}B NMR (96 MHz, acetone-d_6) δ −7.1 ppm; ^{13}C NMR (100 MHz, acetone-d_6) δ 165.8 (qd, J = 49.0 Hz, 3.0 Hz), 162.1 (dq, J = 259 Hz, 4 Hz), 133.4 (m), 120.7 (m), 119.7 (m), 113.3 (J = 25 Hz); ^{19}F NMR (376 MHz, acetone-d_6) δ −114.88 ppm. HRMS (ESI): calcd for $C_{24}H_{12}BBr_4F_4^-$ $[M - K]^-$ 706.7655; found 706.7674.

Potassium tetrakis(4-bromobiphenylyl)borate, THF solvate (6·THF). A slurry of 4,4′-dibromobiphenyl (50.5 g, 160 mmol) in Et_2O (500 mL) was cooled to −20 °C and 2 M *n*-BuLi (80 mL, 160 mmol) was added dropwise while maintaining the temperature below −10 °C. The resulting mixture was stirred for 1 h at −5 °C and then cooled to −78 °C. Then a 1 M solution of BCl_3 in hexane (35 mL, 35 mmol) was added dropwise. Further workup was performed as described for **1**. White powder, dec. >345 °C, yield: 29.5 g (82%). ^{1}H NMR (300 MHz, DMSO-d_6) ^{1}H NMR (400 MHz, DMSO-d_6) δ 7.62–7.56 (m, 16H), 7.44–7.38 (m, 8H), 7.33 (d, J = 8.1 Hz, 8H), 3.62–3.58 (m, 1H), 1.75–1.71 (m, 1H). ^{13}C NMR (101 MHz, DMSO-d_6) δ 163.2 (d, J_{BC} = 49.3 Hz), 141.0, 136.1, 132.4, 131.5, 128.2, 123.9 (q, J_{BC} = 2.8 Hz), 119.3, 67.0, 25.2 ppm. HRMS (ESI): calcd for $C_{48}H_{32}BBr_4^-$ $[M - K]^-$ 938.9284; found 938.9313.

Ammonium tetrakis(4-carboxyphenyl)borate (3a). A solution of **3** (9.0 g, 10.5 mmol) in THF (50 mL) was added to a stirred solution of *t*BuLi (1.7 M solution in pentane, 50 mL, 85 mmol) in THF (150 mL) at −78 °C. The resulting dark-green mixture containing the tetralithio intermediate **3-Li** was stirred for 1 h and cooled to −100 °C. Then it was saturated with dry gaseous CO_2 while maintaining the temperature below −80 °C. The resulting white suspension was allowed to reach room temperature and filtered. The solid was washed with Et_2O (2 × 50 mL) and treated with 20 wt% aq. NH_4Cl (20 mL). The mixture was concentrated under reduced pressure to remove THF and then acidified with aq. HCl (to reach pH of *ca.* 1) resulting in the formation of a viscous material at the bottom of the flask. The supernatant was decanted, whereas the crude product was washed several times with a small portion of cold water (acidified with a few drops of aq. HCl, pH = 3). Then it was mixed with dichloromethane (20 mL) which led to the formation of a white precipitate. The suspension was filtered and the solid was stirred with a mixture of acetone (10 mL) and dichloromethane (20 mL) for 1 h at 0 °C and filtered. The product was dried under reduced pressure to give **3a** as a white powder, dec. >205 °C, yield: 4.8 g (87%). ^{1}H NMR (400 MHz, acetone-d_6) δ 7.68 (d, J = 8.0 Hz, 2H), 7.38–7.33 (m, 2H) ppm; ^{11}B NMR (96 MHz, acetone-d_6) δ −6.5 ppm; ^{13}C NMR (100 MHz, acetone-d_6) δ 170.9, 169.3 (q, J_{BC} = 49 Hz), 135.4 (d, J_{BC} = 2.0 Hz), 127.1 (q, J_{BC} = 2.7 Hz), 126.3 ppm. HRMS (ESI): calcd for $C_{28}H_{20}BO_8^-$ $[M - NH_4]^-$ 495.1245; found 495.1261.

Potassium tetrakis(4-formylphenyl)borate (3b). This compound was obtained from **3** (2.15 g, 2.5 mmol). The lithiate **3-Li** was generated as described for **3a**. It was quenched with DMF (1.8 g, 24.6 mmol). The resulting white suspension was stirred at −78 °C for 30 min and then allowed to warm to room temperature and evaporated under reduced pressure to leave a white solid. It was mixed with Et_2O (50 mL) and the suspension was filtered and the solid was washed with hexane (10 mL) and resuspended in hexane (10 mL). Then the mixture was hydrolyzed aq. KCl (10 wt%, 10 mL) and aq. HCl (4 M, *ca.* 5 mL) was added to reach the pH of *ca.* 3. The obtained yellow slurry was filtered to give a crude product. It was washed with water (2 × 10 mL) and DCM (4 × 5 mL), and dried to give **3b** as a cream-white powder, dec. >220 °C, yield: 0.91 g (77%). ^{1}H NMR (400 MHz, acetone-d_6) δ 9.89 (s, 4H), 7.59 (d, J = 7.9 Hz, 8H), 7.53–7.48 (m, 8H) ppm. ^{13}C NMR (101 MHz, acetone-d_6) δ 192.3, 171.9 (q, J_{BC} = 48.9 Hz), 135.9 (q, J_{BC} = 1.4 Hz), 132.6, 127.3 (q, J_{BC} = 2.8 Hz) ppm. ^{11}B NMR (96 MHz, acetone-d_6) δ −6.00 to −6.20 (m). HRMS (ESI): calcd for $C_{28}H_{20}BO_4^-$ $[M - K]^-$ 431.1449; found 431.1464.

Lithium tetrakis[4-(*N*-*tert*-butylcarbamoyl)phenyl]borate (3c). This compound was obtained from **3** (2.15 g, 2.5 mmol). The lithiate **3-Li** was generated as described for **3a**. It was quenched with *t*-BuNCO (1.98 g, 20.0 mmol). The mixture was stirred at −78 °C for 30 min and then allowed to warm to room temperature. Then it was evaporated to leave a solid residue

which was hydrolyzed with aq. HCl (3 M, *ca.* 10 mL) to reach the pH of *ca.* 3. The viscous residue was washed with water (2 × 10 mL) and triturated with Et_2O (10 mL). The resulting suspension was filtered to give a white solid. It was dissolved in acetone (3 mL) and a mixed solvent (DCM/hexane, 20 mL, 1 : 1) was added. The resulting suspension was concentrated and filtered. The product was washed with DCM (3 mL) and dried to give **3c** as a white powder, dec. >280 °C, yield: 1.45 g (81%). ^{1}H NMR (300 MHz, DMSO-d_6) δ 7.39 (d, J = 8.1 Hz, 8H), 7.34 (s, 4H), 7.25–7.18 (m, 8H), 1.36 (s, 36H) ppm. ^{13}C NMR (101 MHz, DMSO-d_6) δ 168.2, 167.0 (q, J_{BC} = 49.1 Hz), 135.1, 130.5, 125.1, 50.7, 29.2. ^{11}B NMR (96 MHz, DMSO-d_6) δ −6.8 ppm. HRMS (ESI): calcd for $C_{44}H_{56}BN_4O_4^-$ $[M - Li]^-$ 715.4389; found 715.4417.

Ammonium tetrakis[4-(dihydroxyboryl)phenyl]borate (3d). This compound was obtained from **3** (4.3 g, 5.0 mmol). The lithiate **3-Li** was generated as described for **3a**. It was quenched with $B(OMe)_3$ (5.6 g, 6 mL, 55 mmol). The mixture was stirred at −78 °C for 30 min and then allowed to warm to room temperature. Then it was evaporated to leave a white solid residue. It was treated with aq. $Na_2S_2O_5$ (10 wt%, 2 mL), aq. NH_4Cl (20 wt%, 10 mL) and the pH was adjusted to the value of *ca.* 3–4 by the addition of aq. HCl. The mixture was evaporated to dryness and the obtained solid was triturated with methanol (20 mL). The suspension was filtered and the filtrate was evaporated. The crude solid product was washed with cold water (5 mL) and dichloromethane (5 mL) and dried to give **3c** as a white powder, dec. >340 °C, yield: 1.4 g (53%). ^{1}H NMR (400 MHz, acetone-d_6) δ 7.47 (d, J = 9.0 Hz, 8H), 7.35–7.31 (m, 8H) ppm; ^{13}C NMR (100 MHz, acetone-d_6) δ 167.5 (q, J_{BC} = 49 Hz), 135.4 (q, J_{BC} = 2.0 Hz), 131.4 (q, J_{BC} = 2.7 Hz), 125.0 ppm; ^{11}B NMR (96 MHz, acetone-d_6) δ 28.4, −6.6 ppm. HRMS (ESI): calcd for $C_{24}H_{24}B_5O_8^-$ $[M - NH_4]^-$ 494.1967; found 494.1985.

Lithium tetrakis(3-carboxyphenyl)borate (4a). This compound was obtained as described for **3a** starting with **4** (2.15 g, 2.5 mmol). Due to a significant solubility of **4a** in water, the reaction mixture obtained after addition of 4 M aq. HCl was evaporated to dryness and the solid residue was extracted with acetone (30 mL). The extract was concentrated and then dichloromethane was added to precipitate the product as a white powder. Elemental analysis revealed that the product was obtained as a lithium salt contaminated with some amount of potassium (*ca.* 10%). White powder, dec. >190 °C, yield: 0.9 g (68%). ^{1}H NMR (400 MHz, acetone-d_6) δ 8.07 (s, 1H), 7.55 (d, J = 7.6 Hz, 1H), 7.48 (s, 1H), 7.05 (td, J = 7.5, 3.9 Hz, 1H) ppm; ^{13}C NMR (101 MHz, acetone-d_6) δ 171.8, 162.7 (q, J_{BC} = 49.5 Hz), 140.1, 136.8, 129.6, 125.6, 124.0. ^{11}B NMR (96 MHz, acetone-d_6) δ −6.7 ppm; HRMS (ESI): calcd for $C_{28}H_{20}BO_8^-$ $[M - Li]^-$ 495.1245; found 495.1263.

Lithium tetrakis[3-(*N-tert*-butylcarbamoyl)phenyl]borate (4b). This compound was obtained as described for **3c** starting with **4** (1.08 g, 1.25 mmol). The product was isolated as the acetone solvate. White powder, dec. >222 °C, yield: 0.75 g (78%). ^{1}H NMR (300 MHz, DMSO-d_6) δ 7.62 (s, 4H), 7.26 (d, J = 7.0 Hz, 4H), 7.09 (s, 4H), 7.01 (t, J = 7.4 Hz, 4H), 2.09 (s, 6H), 1.32 (s, 36H) ppm. ^{13}C NMR (101 MHz, DMSO-d_6) δ 206.9, 167.0, 162.7 (q, J_{BC} = 49.5 Hz), 138.8, 134.4, 133.7 (q, J_{BC} = 2.8 Hz), 125.4, 121.6, 50.7, 31.1, 29.1 ppm. ^{11}B NMR (96 MHz, DMSO-d_6) δ −6.7 ppm. HRMS (ESI): calcd for $C_{44}H_{56}BN_4O_4^-$ $[M - Li]^-$ 715.4389; found 715.4413.

Ammonium tetrakis(4-carboxybiphenylyl)borate (6a). A solution of **6** (4.8 g, 5.0 mmol) in THF (25 mL) was added to a stirred solution of *t*BuLi (1.7 M solution in pentane, 25 mL, 42 mmol) in THF (70 mL) at −78 °C. The resulting dark-blue mixture containing the tetralithio intermediate **6-Li** was stirred for 1 h. Carboxylation with gaseous CO_2 and further workup was carried out as described for analogous compound **3a**. White powder, dec. >202 °C, yield: 2.9 g (73%). ^{1}H NMR (400 MHz, DMSO-d_6) δ 12.78 (broad, 4H), 7.94 (d, J = 8.5 Hz, 8H), 7.76–7.70 (m, 8H), 7.41 (s, 16H) ppm. ^{13}C NMR (101 MHz, DMSO-d_6) δ 167.8, 164.3 (q, J_{BC} = 49 Hz), 146.4, 136.5, 132.9, 130.3, 128.7, 126.4, 124.8 ppm. ^{11}B (96 MHz, DMSO-d_6) −7.0 ppm. HRMS (ESI): calcd for $C_{52}H_{36}BO_8^-$ $[M - NH_4]^-$ 799.2498; found 799.2522.

Potassium tetrakis(4-formylbiphenylyl)borate (6b). This compound was obtained as described for **3b** starting with **6** (4.8 g, 5.0 mmol). Yellow powder, dec. >205 °C, yield: 2.5 g (68%). ^{1}H NMR (400 MHz, DMSO-d_6) δ 9.98 (s, 4H), 7.91 (d, J = 8.2 Hz, 8H), 7.85 (d, J = 8.2 Hz, 8H), 7.48–7.44 (m, 16H) ppm. ^{13}C NMR (101 MHz, DMSO-d_6) δ 193.0, 164.7 (q, J_{BC} = 49.0 Hz), 148.1, 136.6, 134.5, 132.8, 130.6, 127.0, 125.0 ppm. ^{11}B NMR (96 MHz, DMSO-d_6) δ −6.8 ppm. HRMS (ESI): calcd for $C_{52}H_{32}BO_8^-$ $[M - K]^-$ 735.2701; found 735.2724.

Lithium tetrakis[4-(*N-tert*-butylcarbamoyl)biphenylyl]borate (6c). This compound was obtained as described for **3c** starting with **6** (2.4 g, 2.5 mmol). The product was isolated as a white powder, dec. >255 °C, yield: 0.91 g (78%). ^{1}H NMR (300 MHz, DMSO-d_6) δ 7.83 (d, J = 8.4 Hz, 8H), 7.71 (d, J = 8.8 Hz, 8H), 7.67 (s, 4H), 7.46–7.36 (m, 16H), 1.40 (s, 36H) ppm. ^{13}C NMR (101 MHz, DMSO-d_6) δ 166.7, 163.9 (q, J_{BC} = 47.5 Hz), 144.5, 136.5, 133.8, 133.2, 128.3, 125.9, 124.6, 51.1, 29.1 ppm. ^{11}B NMR (96 MHz, DMSO-d_6) δ −6.8 ppm. HRMS (ESI): calcd for $C_{68}H_{72}BN_4O_4^-$ $[M - Li]^-$ 1019.5652; found 1019.5674.

Potassium tetrakis(4-(dihydroxyboryl)biphenylyl)borate (6d). This compound was obtained as described for **3c** starting with **6** (2.4 g, 2.5 mmol). However, the mixture obtained after addition with $B(OMe)_3$ was warmed to room temperature and quenched with Me_3SiCl (3 mL). The resultant solution was stirred for 1 h and evaporated under reduced pressure to leave a pale yellow waxy residue. DCM (50 mL) was added and the obtained suspension was stirred for 30 min and filtered under argon. The filtrate was evaporated to dryness and the resulting solid was treated with aq. KCl (10 wt%, 20 mL). Acetone (20 mL) was added to dissolve any remaining solid and the mixture was concentrated to remove organic solvents. The aqueous phase was decanted from over the precipitated waxy material. It was washed with water (3 × 5 mL) and DCM (20 mL) was added. The obtained slurry was stirred for 2 h and the product was filtered, washed with DCM (3 × 5 mL) and dried to give white powder, dec. >370 °C, yield: 1.55 g (77%). ^{1}H NMR (400 MHz, DMSO-d_6) δ 8.06 (s, $B(OH)_2$, 8H), 7.85

(d, J = 7.2 Hz, 8H), 7.62 (d, J = 7.1 Hz, 8H), 7.46–7.36 (m, 16H) ppm. ^{13}C NMR (101 MHz, DMSO-d_6) δ 163.5 (q, J_{BC} = 49.4 Hz), 143.7, 136.5, 135.1, 134.0, 129.1, 126.6, 125.5, 124.5 ppm. ^{11}B NMR (MHz, DMSO-d_6) δ 28.0, −7.5 ppm. HRMS (ESI): calcd for $C_{48}H_{40}BO_8^-$ $[M - K]^-$ 798.3219; found 799.3239. Note: The standard workup involving hydrolysis with an aqueous HCl product was not effective and the formation of the 4-biphenylboronic acid by-product was observed to a varying extent. Presumably **6d** is quite unstable at the lower pH (below 2–3) due to the cleavage of B–C bonds at the quaternary boron centre.

X-ray structural measurement and refinement details

The single crystals of **3c**, **3d** and **4a** were obtained by slow evaporation of the corresponding mixed acetone–water solutions. They were measured at 100 K on a SuperNova diffractometer equipped with an Atlas detector (Cu-K$_\alpha$ radiation, λ = 1.54184 Å). Data reduction and analysis were carried out with the CrysAlisPro program.[39] All structures were solved by direct methods using SHELXS-97[40] and refined using SHELXL-2014.[41]

Despite the fact that the measured diffraction data of **4a** is of good quality (R_{int} < 3.0%), the final R ad wR_2 refinement factors for this structure are of 13.81% and 38.5% ($I \geq 3\sigma(I)$). This is because of the poor description of the solvent molecules located in the crystal cavities. We have found that at least three different solvent molecules may be presented in the network voids including (a) acetone (not included in the refinement), (b) the product of its aldol condensation – 4-hydroxy-4-methylpentan-2-one, and (c) 4-methylpent-3-en-2-one – the dehydration product of the latter compound. Due to the geometrical similarity of all solvent molecules, their positions in the structure may overlap. This is especially noticeable for 4-methylpent-3-en-2-one, in which C=C sp^2 carbon atom is slightly pyramidilized, and some residual electron density was found in the direction perpendicular to the molecular plane (1.03 e Å^{-3}) suggesting the presence of other atoms close to the C=C sp^2 carbon atom (probably oxygen atom with partial occupation). However, the 4-hydroxy-4-methylpentan-2-one does not fit as well and we were unable to find a more reliable model to describe the solvent disorder. All atoms of disordered solvent molecules were refined isotropically with the site occupancy factors fixed at the exact values of 0.5. Furthermore, we have found that the lithium cations are disordered over 4 different positions (see Fig. S31 SI†). The presence of lithium cations was confirmed by atomic absorption spectroscopy analysis (AAS). The removal of all solvent molecules and lithium cations followed by the SQUEEZE procedure resulted in the decrease of the R ad wR_2 refinement factors to 4.48% and 12.0%, respectively, showing that, indeed, most of the refinement problems are related to the improper description of molecular species located in crystal cavities. Both crystallographic models (**4a** and **4a_squeeze**) are provided in the ESI.† Besides the solvent disorder, two carboxylic groups from COOH···HOOC dimers were also found to be disordered over two positions each, probably being the result of the rotation of the 3-carboxyphenyl group along the B–C bond by small angle. For the better description of the position of disordered atoms, the same anisotropic displacement parameters were used (EADP instruction). Furthermore, the O1A and O1B atoms were restrained so that their U_{ij} components approximate to isotropic behavior (ISOR instruction). In the case of the model with fully refined solvent molecules, several reflections were omitted as their observed and calculated F^2 values disagree significantly.

In the case of **3c**, the diffraction was not observed at a higher theta (θ > 50°) angle even after prolonged data acquisition (180 s per frame). Furthermore, the structure contains disordered solvent molecules located inside the crystal pores. According to the SQUEEZE procedure, these correspond to 2 molecules of acetone. The disordered solvent molecules were masked using OLEX software.[42]

The compound **3d** crystallizes in the form of very tiny crystals. Thus the diffraction was not observed at higher theta angle (θ > 50°) and it was not measured.

Crystallographic Information Files (CIFs) have been deposited with the Cambridge Crystallographic Data Centre as supplementary publications no. 1840090 (**3d**),† 1841321 (**3c**) and 1840091 (**4a**).

Crystal data for 3c. $C_{44}H_{52}BN_4O_4Li{\cdot}2C_3H_6O$, M_r = 838.83 a.u.; monoclinic; $P2_1/c$; a = 17.560(3) Å, b = 22.0645(18) Å, c = 16.8909(18) Å, β = 114.517(15)°, V = 5954.4(13) Å^3; d_{calc} = 0.933 g cm^{-3}; μ = 0.474 mm^{-1}; Z = 4; F(000) = 1803; number of collected/unique reflection (R_{int} = 9.19%) = 16 879/6449, R[F]/wR[F] ($I \geq 3\sigma(I)$) = 8.01%/18.63%, $\Delta\varrho_{res}^{(min/max)}$ = −0.226/+0.270 e Å^{-3}.

Crystal data for 3d. $C_{24}H_{24}B_5O_8NH_4{\cdot}4(H_2O)$, M_r = 583.58 a.u.; orthorhombic; $Pnn2$; a = 14.1966(9) Å, b = 8.5378(8) Å, c = 11.9968(16) Å, V = 1454.1(3) Å^3; d_{calc} = 1.335 g cm^{-3}; μ = 0.854 mm^{-1}; Z = 2; F(000) = 990; number of collected/unique reflection (R_{int} = 5.54%) = 2573/1009, R[F]/wR[F] ($I \geq 3\sigma(I)$) = 6.84%/19.75%, $\Delta\varrho_{res}^{(min/max)}$ = −0.26/+0.26 e Å^{-3}.

Crystal data for 4a. $C_{28}H_{20}BO_8LiC_6H_{12}O_2{\cdot}0.5C_6H_{10}O$, M_r = 667.41 a.u.; monoclinic; $P2_1/n$; a = 15.1982(11) Å, b = 17.4686(5) Å, c = 17.705(2) Å, β = 101.258(14)°, V = 4610.0(7) Å^3; d_{calc} = 0.962 g cm^{-3}; μ = 0.572 mm^{-1}; Z = 4; F(000) = 1404; number of collected/unique reflection (R_{int} = 2.75%) = 33 268/7059, R[F]/wR[F] ($I \geq 3\sigma(I)$) = 13.81%/38.47%, $\Delta\varrho_{res}^{(min/max)}$ = −0.364/+1.220 e Å^{-3}. Squeeze: R[F]/wR[F] ($I \geq 3\sigma(I)$) = 4.48%/12.0%, $\Delta\varrho_{res}^{(min/max)}$ = −0.217/+0.263 e Å^{-3}.

Conflicts of interest

There are no conflicts to declare.

Acknowledgements

This work was supported by National Science Centre (Poland) within the framework of the project DEC-UMO-2016/21/B/ST5/00118. X-ray measurements were performed in the Crystallographic Unit of the Physical Chemistry Laboratory at the Chemistry Department of the University of Warsaw.

References

1 E. Bakker, P. Bühlmann and E. Pretsch, *Chem. Rev.*, 1997, **97**, 3083–3132.
2 J. Bobacka, T. Alaviuhkola, V. Hietapelto, H. Koskinen, A. Lewenstam, M. Lämsä, J. Pursiainen and A. Ivaska, *Talanta*, 2002, **58**, 341–349.
3 J. Bobacka, V. Väänänen, A. Lewenstam and A. Ivaska, *Talanta*, 2004, **63**, 135–138.
4 G. Lu, R. Franzén, Q. Zhang and Y. Xu, *Tetrahedron Lett.*, 2005, **46**, 4255–4259.
5 R. Shintani, Y. Tsutsumi, M. Nagaosa, T. Nishimura and T. Hayashi, *J. Am. Chem. Soc.*, 2009, **131**, 13588–13589.
6 G.-R. Qu, P.-Y. Xin, H.-Y. Niu, X. Jin, X.-T. Guo, X.-N. Yang and H.-M. Guo, *Tetrahedron*, 2011, **67**, 9099–9103.
7 T. Matsuda, K. Mizuno and S. Watanuki, *J. Organomet. Chem.*, 2014, **765**, 64–67.
8 J. Broeke, Arylborate Anions; Versatile Counterions, in *Homogeneous Catalysis with Potential for Use in Novel Reaction Media*, Utrecht, Netherlands, 2000.
9 E. Y.-X. Chen and T. J. Marks, *Chem. Rev.*, 2000, **100**, 1391–1434.
10 T. J. Herrington, A. J. W. Thom, A. J. P. White and A. E. Ashley, *Dalton Trans.*, 2012, **41**, 9019–9022.
11 P. K. Bakshi, A. Linden, B. R. Vincent, S. P. Roe, D. Adhikesavalu, T. S. Cameron and O. Knop, *Can. J. Chem.*, 1994, **72**, 1273–1293.
12 P. K. Bakshi, T. S. Cameron and O. Knop, *Can. J. Chem.*, 1996, **74**, 201–220.
13 U. Behrens, F. Hoffmann and F. Olbrich, *Organometallics*, 2012, **31**, 905–913.
14 S. Kiviniemi, M. Nissinen, T. Alaviuhkola, K. Rissanen and J. Pursiainen, *J. Chem. Soc., Perkin Trans. 2*, 2001, **12**, 2364–2369.
15 T. Alaviuhkola, J. Bobacka, M. Nissinen, K. Rissanen, A. Ivaska and J. Pursiainen, *Chem. – Eur. J.*, 2005, **11**, 2071–2080.
16 J. F. van Humbeck, M. L. Aubrey, A. Alsbaiee, R. Ameloot, G. W. Coates, W. R. Dichte and J. R. Long, *Chem. Sci.*, 2015, **6**, 5499–5505.
17 F. P. Cassaretto, J. J. McLafferty and C. E. Moore, *Anal. Chim. Acta*, 1965, **32**, 376–380.
18 R. Anulewicz-Ostrowska, T. Kliś, D. Krajewski, B. Lewandowski and J. Serwatowski, *Tetrahedron Lett.*, 2003, **44**, 7329–7331.
19 N. A. Yakelis and R. G. Bergman, *Organometallics*, 2005, **24**, 3579–3581.
20 N. Malek, M. Saied and J. D. Wuest, *J. Soc. Chim. Tunis.*, 2006, **8**, 55–61.
21 N. Malek, T. Maris, M. Simard and J. D. Wuest, *J. Am. Chem. Soc.*, 2005, **127**, 5910–5916.
22 Y. Yamamoto, T. Seko and H. Nemoto, *J. Org. Chem.*, 1989, **54**, 4734–4736.
23 P. Vedsø, P. H. Olesen and T. Hoeg-Jensen, *Synlett*, 2004, 892–894.
24 P. Kurach, S. Luliński and J. Serwatowski, *Eur. J. Org. Chem.*, 2008, 3171–3178.
25 G. Wesela-Bauman, L. Jastrzębski, P. Kurach, S. Luliński, J. Serwatowski and K. Woźniak, *J. Organomet. Chem.*, 2012, **711**, 1–9.
26 J.-H. Fournier, T. Maris, J. D. Wuest, W. Guo and E. Galoppini, *J. Am. Chem. Soc.*, 2003, **125**, 1002–1006.
27 A. P. Coté, A. I. Benin, N. W. Ockwig, M. O'Keeffe, J. Matzger and O. Yaghi, *Science*, 2005, **310**, 1166–1170.
28 H. M. El-Kaderi, J. R. Hunt, J. L. Mendoza-Cortes, A. P. Coté, R. E. Taylor, M. O'Keeffe and O. M. Yaghi, *Science*, 2007, **316**, 268–272.
29 E. Ihara, V. G. Young and R. F. Jordan, *J. Am. Chem. Soc.*, 1998, **120**, 8277–8278.
30 T. Li, A. J. Lough, C. Zuccaccia, A. Macchioni and R. H. Morris, *Can. J. Chem.*, 2006, **84**, 164–175.
31 U. Olsher, R. M. Izatt, J. S. Bradshaw and N. K. Dalley, *Chem. Rev.*, 1991, **91**, 137–164.
32 T. Steiner and S. A. Mason, *Acta Crystallogr., Sect. B: Struct. Sci.*, 2000, **56**, 254–260.
33 M. Dąbrowski, K. Durka, S. Luliński, J. Serwatowski and J. Warkocka, *Acta Crystallogr., Sect. E: Struct. Rep. Online*, 2011, **67**, o3098.
34 K. Durka, K. N. Jarzembska, R. Kamiński, S. Luliński, J. Serwatowski and K. Woźniak, *Cryst. Growth Des.*, 2012, **12**, 3720–3734.
35 I. D. Madura, K. Czerwińska and D. Sołdańska, *Cryst. Growth Des.*, 2014, **14**, 5912–5921.
36 N. Malek, T. Maris, M. Simard and J. D. Wuest, *Acta Crystallogr., Sect. E: Struct. Rep. Online*, 2005, **61**, o518–o520.
37 Y.-B. Men, J. Sun, Z.-T. Huang and Q.-Y. Zheng, *CrystEngComm*, 2009, **11**, 978–979.
38 J. B. Lambert, Y. Zhao and C. L. Stern, *J. Phys. Org. Chem.*, 1997, **10**, 229–232.
39 *CrysAlis Pro Software*, Oxford Diffraction Ltd., Oxford, U.K., 2010.
40 G. M. Sheldrick, *Acta Crystallogr., Sect. A: Found. Crystallogr.*, 2008, **64**, 112–122.
41 G. M. Sheldrick, *Acta Crystallogr., Sect. C: Struct. Chem.*, 2015, **71**, 3–8.
42 O. V. Dolomanov, L. J. Bourhis, R. J. Gildea, J. A. K. Howard and H. Puschmann, *J. Appl. Crystallogr.*, 2009, **42**, 339–341.